Optical Kaleidoscope Using a Single Atom

P. Horak and H. Ritsch
Institut für Theoretische Physik, Universität Innsbruck, Technikerstrasse 25, A-6020 Innsbruck, Austria

T. Fischer, P. Maunz, T. Puppe, P. W. H. Pinkse, and G. Rempe
Max-Planck-Institut für Quantenoptik, Hans-Kopfermann-Strasse 1, D-85748 Garching, Germany
(Received 11 May 2001; published 9 January 2002)

A new method to track the motion of a single particle in the field of a high-finesse optical resonator is analyzed. It exploits sets of near-degenerate higher-order Gaussian cavity modes, whose symmetry is broken by the position dependent phase shifts induced by the particle. Observation of the spatial intensity distribution outside the cavity allows direct determination of the particle's position. This is demonstrated by numerically generating a realistic atomic trajectory using a semiclassical simulation and comparing it to the reconstructed path. The path reconstruction itself requires no knowledge about the forces on the particle. Experimental realization strategies are discussed.

DOI: 10.1103/PhysRevLett.88.043601 PACS numbers: 42.50.Ct, 32.80.Pj, 42.50.Vk

In a variety of pioneering experiments in the past few years [1–3] it has been demonstrated and widely exploited that a single near-resonant atom can significantly influence the field dynamics in a microscopic high-finesse optical resonator. Vice versa, the light field also influences the motion of a cold atom, which leads to an intricate dynamical interplay of atomic motion and field dynamics [4,5]. As a striking example, trapping of a single atom in the field of a single photon has become feasible [6,7]. This was experimentally substantiated by analyzing the characteristics of the measured output field. The time variation of the transmitted intensity shows very good agreement with theoretical simulations [8] of the confined three-dimensional motion of the atom in the cavity light field including friction and diffusion [9–11]. Carrying this analysis further it was even possible to associate piecewise reconstructed trajectories with recorded time-dependent intensity curves [7,12], utilizing the knowledge of the near-conservative potential. However, the reconstruction was possible only for atoms with sufficiently large and conserved angular momentum around the cavity axis and can be done only up to an overall angle and the direction of rotation. The reason was that only a single cavity mode, the TEM_{00} mode, was used. Consequently, only a single spatial degree of freedom of the atom could be extracted directly from a measurement of the transmitted field.

In this Letter we investigate a new method to obtain two-dimensional position information on the atom using near frequency-degenerate higher-order transverse modes. Examples are the Hermite-Gaussian (HG) or the Laguerre-Gaussian (LG) modes, which possess a rectangular matrix of intensity minima and maxima or a pattern of concentric rings in the transverse plane. The atom inside the resonator redistributes photons from one mode to the other and tends to phase lock them. Moreover, it induces frequency shifts and losses dependent on its position. In total, the symmetry of the intracavity field determined by cavity and pump geometry is perturbed and characteristic optical patterns containing information on the atomic position appear. These patterns are reminiscent of a toy kaleidoscope in which small objects in a symmetric arrangement of mirrors create images of a given symmetry. Our technique yields much more information on the atomic position and motion as compared to the single-mode case and allows extraction of the atomic position from a measurement of the field pattern.

To treat this problem quantitatively we generalize previous semiclassical models of dynamical cavity QED to include finite sets of nearly degenerate eigenmodes. For a weakly saturated atom we derive a coupled set of equations for the mode amplitudes and the atomic center-of-mass motion. To be specific, let us consider a single two-level atom with transition frequency ω_a and linewidth Γ (half width at half maximum) moving inside a high-finesse optical resonator with transversal LG eigenmodes $u_{pm}(\mathbf{r})$, where p is the radial mode index and m is the azimuthal mode index [13],

$$u_{pm}(\rho,\theta,z) = C_{pm}\cos(kz)e^{-(\rho^2/\mathrm{w}_0^2)+im\theta} \times (-1)^p\left(\frac{\rho\sqrt{2}}{\mathrm{w}_0}\right)^{|m|} L_p^{|m|}\left(\frac{\sqrt{2}\,\rho^2}{\mathrm{w}_0^2}\right), \quad (1)$$

where L_n^α is the generalized Laguerre polynomial. The normalization parameters, C_{pm}, are chosen such that $\int |u_{pm}(\rho,\theta,z)|^2\,dV = d\mathrm{w}_0^2\pi/4 = V_{00}$ (the TEM_{00} mode volume), where w_0 is the cavity waist and d the cavity length. At each spatial point the local atom-mode couplings are $g_{pm}(\mathbf{r}) = g_0 u_{pm}(\mathbf{r})$, where g_0 is the maximum coupling of the TEM_{00} mode. The electric field is given by $\sum_{pm}\alpha_{pm}u_{pm}(\mathbf{r})$, where α_{pm} is the amplitude of the mode u_{pm}. For simplicity, we assume that the mirrors are ideally spherical and have a uniform coating. Then, all these modes have a common eigenfrequency ω and field decay rate κ. However, the model can be extended to incorporate nondegenerate modes in a straightforward manner. The cavity is assumed short compared to the

Rayleigh length of the mode so that the wave fronts are approximately plane with z dependence $\cos(2\pi z/\lambda)$. The resonator is externally driven by a coherent pump field of frequency ω_p which pumps the modes with strengths η_{pm}. Assuming low atomic saturation, we can adiabatically eliminate the internal atomic dynamics and treat the atom as a linearly polarizable particle, which induces a spatially dependent phase shift and loss. In the semiclassical limit, where we consider the center-of-mass motion of the atom classically, we can derive the following set of coupled differential equations for the mode amplitudes $\alpha_{pm}(t)$, the atomic position $\mathbf{r}_a(t)$, and momentum $\mathbf{p}_a(t)$ [14]:

$$\dot{\mathbf{r}}_a = \frac{\mathbf{p}_a}{M}, \qquad \dot{\mathbf{p}}_a = -U_0 \sum_{m,n} \nabla[u_{pm}(\mathbf{r}_a) u^*_{pn}(\mathbf{r}_a)]\alpha_{pm}\alpha^*_{pn} + i\gamma \times \sum_{m,n} [u_{pm}(\mathbf{r}_a)\nabla u^*_{pn}(\mathbf{r}_a) - u^*_{pn}(\mathbf{r}_a)\nabla u_{pm}(\mathbf{r}_a)]\alpha_{pm}\alpha^*_{pn} + \chi,$$

$$\dot{\alpha}_{pm} = \eta_{pm} + (i\Delta - \kappa)\alpha_{pm} - (iU_0 + \gamma)u_{pm}(\mathbf{r}_a)\sum_n u^*_{pn}(\mathbf{r}_a)\alpha_{pn} + \xi_{pm}. \quad (2)$$

Here, M is the atomic mass, $U_0 = \delta g_0^2/(\delta^2 + \Gamma^2)$ with $\delta = \omega_p - \omega_a$ the single-photon optical light shift, $\gamma = \Gamma g_0^2/(\delta^2 + \Gamma^2)$ the spontaneous emission rate for a single-photon field, $\Delta = \omega_p - \omega$ the cavity-pump detuning, and χ and ξ_{pm} are Gaussian random variables which model momentum and cavity field fluctuations, respectively.

For an atom at rest one can solve Eqs. (2) for the mean stationary field amplitudes $\alpha^{\text{stat}}_{pm}(\mathbf{r}_a)$, which in a parametric way depend on the atomic position $\mathbf{r}_a$. We get

$$\alpha^{\text{stat}}_{pm}(\mathbf{r}_a) = \frac{\eta^*_{pm}}{i\Delta - \kappa} + \frac{iU_0 + \gamma}{i\Delta - \kappa} u^*_{pm}(\mathbf{r}_a)\mathcal{E}_0(\mathbf{r}_a), \quad (3)$$

where $\mathcal{E}_0$ is the electric field at the position of the atom,

$$\mathcal{E}_0(\mathbf{r}_a) = \frac{\sum_{p,m} u_{pm}(\mathbf{r}_a)\eta^*_{pm}}{(i\Delta - \kappa) - (iU_0 + \gamma)\sum_{p,m} |u_{pm}(\mathbf{r}_a)|^2}. \quad (4)$$

Note that the list of the values of the mode functions at the position of the atom $u_{pm}(\mathbf{r}_a)$ may be seen as coordinates of a vector, which can be rotated into the form $[u_{\text{eff}}(\mathbf{r}_a), 0, 0, \ldots]$. Since any linear combination of the modes can be considered as a mode as well, the atom-field dynamics for an atom at rest thus reduces to the case of a single effective mode u_{eff}. This allows one to derive simple analytical expressions for the steady state. For a moving atom, this approach must be generalized, but still helps in finding analytical expressions for friction and diffusion coefficients for the atomic motion [15].

Let us now consider the family of three degenerate cavity modes with $(p, m) = (1, 0), (0, -2), (0, 2)$. Figure 1 shows the steady state field intensities for the empty cavity and for two different atomic positions. For the chosen parameters [rubidium atoms, $(g_0, \Gamma, \kappa) = 2\pi \times (16, 3, 1.5)$ MHz, $(\eta_{10}, \eta_{0-2}, \eta_{02}) = 2\pi \times (6.4, 0, 0)$MHz, $\Delta = -2\pi \times 2.25$ MHz, and $\delta = -2\pi \times 114$ MHz, leading to $U_0 = \Delta$, $\gamma = 2\pi \times 60$ kHz] the atom distributes photons between the cavity modes and changes their relative phases in such a way that a local maximum of the spatial field intensity pattern is created near the position of the atom. By a change of the detuning between the pump laser, the cavity modes, and the atomic transition, a local minimum can also be achieved. Figure 1 shows the effect of the atom position on the shape and overall intensity of the stationary field distribution.

This dependence of the cavity field on the atomic position suggests that measuring the cavity output field distribution yields ample information on the atomic motion. In

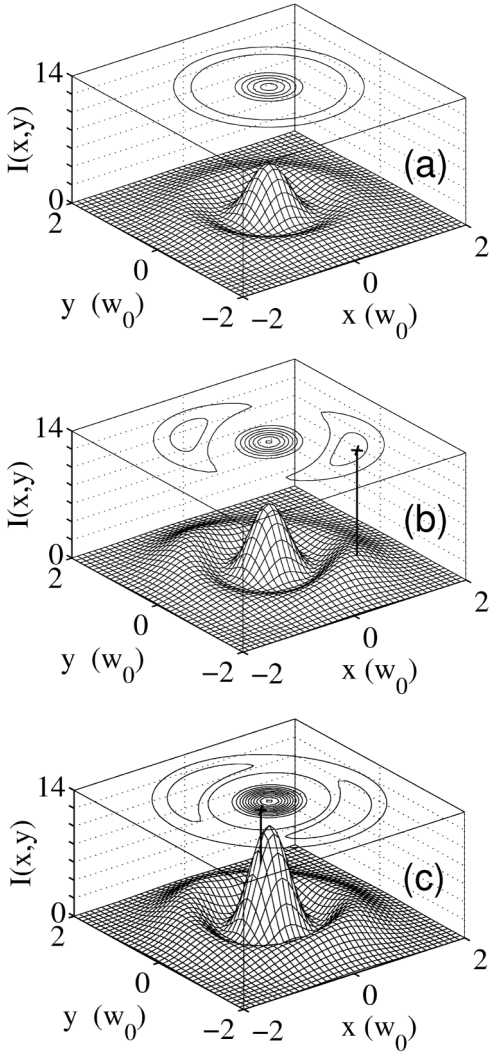

FIG. 1. Transversal spatial intensity pattern of the stationary cavity field for the empty cavity (a) and two atomic positions indicated by the thick vertical line and a cross (b), (c).

fact, it can be shown that the functions $\alpha_{pm}^{\mathrm{stat}}(\mathbf{r}_a)$ can be inverted almost everywhere to yield the atomic position in three dimensions. Of course, one is limited by the common symmetries of all modes. For instance, for the system considered in Fig. 1, a 180° rotation around the cavity axis forms a symmetry operation. Hence, the reconstruction of the atomic position from the cavity field will always yield two equivalent positions. Other symmetry operations are a shift of $\lambda/2$ in the direction of the cavity axis and a reflection at the nodes or antinodes of the standing wave. Another limitation is that an atom cannot be detected close to the (transversal) nodes of the pumped mode (see Fig. 1a). However, it is possible to determine directly from the photodetector signals whether the atomic position can be obtained or not: reconstruction is possible if the transmission signal with an atom differs from the signal of an empty cavity. Also, the nodal areas are small and one is free to alternate rapidly between different pump geometries. Alternatively, one can change the pump geometry online when the atom approaches the nodal area of the pumped mode.

Although in principle a full three-dimensional atomic trajectory can be reconstructed, the method encounters some complications. The longitudinal motion is in general too fast to be resolved experimentally. This amounts to replacing the coupling constant g_0^2 by its longitudinally averaged value. A two-dimensional reconstruction still works in this case, even if the precise factor by which the coupling is reduced is unknown. Second, a single atom must redistribute enough photons among the cavity modes. This requires values of U_0 of the order of the cavity field decay rate κ and hence the strong-coupling regime of cavity QED. In this regime, the coherent coupling of the atom to the cavity mode is larger than the decay constants of the atomic dipole and the cavity field $g_0 > (\kappa, \Gamma)$, requiring a small high-finesse cavity. Third, our arguments above are based on a stationary cavity field. For an atom moving in the xy plane, we thus have to assume that the cavity field follows the transverse atomic motion adiabatically. This implies slow atomic motion and not too large optical forces. For strong coupling this is tantamount to low intracavity photon numbers. The limitations are strongly reduced in systems where the atom is held in place by other forces, as, e.g., in ion traps. Fourth, in an actual experiment the exact intracavity photon number can be deduced only from the number of photons emitted by the cavity, which is subject to statistical fluctuations (shot noise). These become significant in the weak field case limiting the accuracy to which the cavity field and the atomic position can be determined.

Despite all this we will now demonstrate with a realistic sample trajectory that all of these conditions can be met and a numerical reconstruction of the atomic path should be possible using existing optical resonators [6,7]. For simplicity we assume a quasi-two-dimensional situation where the atom is trapped longitudinally close to an antinode ($z = 0$) of the standing wave during the interaction time.

In a first step we create a sample trajectory for a single atom traversing the resonator by integrating the stochastic equations of motion (2) for a given initial atomic position and velocity. This procedure includes all reactive and dissipative optical forces which the cavity field imposes on the atom [14], the backaction of the atom on the cavity field, as well as the momentum and cavity field diffusion. A resulting trajectory is depicted by the solid curve in Fig. 2. The atom enters the resonator from below. By chance, the atom encircles the cavity axis a few times before it is ejected again.

The generated trajectory allows simulation of a realistic cavity output signal. We assume an arrangement of 16 photodetectors at the cavity output port each counting the numbers of photons detected in equally sized sectors covering an angle of 22.5°. Because of the symmetry of the system, the signals from opposing detectors can be added without loss of information. We integrate the simulated photon counts at each detector over a time interval of 100 cavity decay times $1/\kappa$ to obtain the photon flux. For two out of the eight pairs of photodetectors it is shown in Fig. 3.

We will now use only the generated fluxes to reconstruct the atomic trajectory. First, for each time step we determine the most probable atomic position by a least-square comparison with a list of precalculated detector outputs corresponding to the steady-state field distribution $\alpha_{pm}^{\mathrm{stat}}(\mathbf{r}_a)$ for given atomic positions on a discrete grid. Because of the twofold spatial symmetry, we always obtain two equivalent points in that way. From a chosen initial point we select the points forming a continuous curve as a function of time. The spatial points obtained in that way are indicated by the crosses in Fig. 2. For the pump geometry chosen here, the field has a ring-shaped field node, where the atom does not couple to the pumped

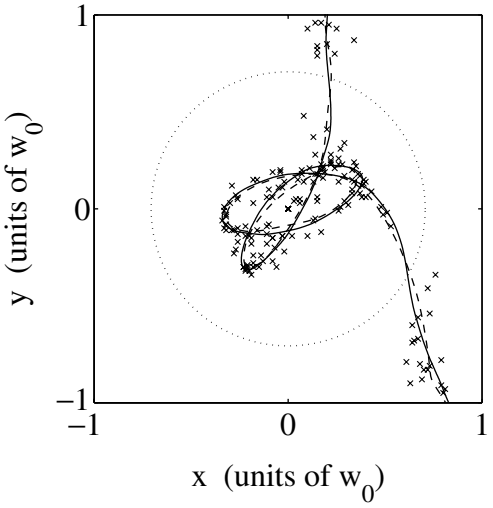

FIG. 2. Central part of Fig. 1(a) with the simulated atomic trajectory (solid curve), reconstructed atomic positions (crosses), and fitted atomic path (dashed curve). The atom enters with a velocity of 12 cm/s and the total trajectory takes 5300 $\kappa^{-1} =$ 0.56 ms. The dashed circle indicates the dark ring of the pumped cavity mode u_{10}. The waist of the TEM_{00} mode is $w_0 = 29$ μm.

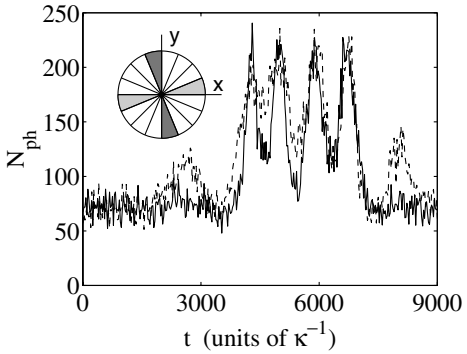

FIG. 3. Simulated photon flux (number of photons N_{ph} per 100 κ^{-1}) measured at two out of 8 photodetector pairs as a function of time (units of κ^{-1}). The inset depicts the arrangement of the detectors on the cavity output, shaded areas correspond to the plotted curves.

modes. Close to this ring, the reconstruction is difficult. In principle there are ways around this problem, but here the corresponding crosses are simply left out.

Because of shot noise in the measured photon fluxes (Fig. 3), the reconstructed atomic positions show a certain spatial spread. Since for the given parameters the momentum diffusion in Eqs. (2) is small compared to the dipole force, we fit a smooth curve to the discrete set of data. The resulting reconstructed trajectory is shown by the dashed curve in Fig. 2. Note that rotation by 180° forms an equivalent solution, which can be selected by choosing an alternative initial condition. Comparing the reconstructed with the original trajectory we note that for the depicted area close to the cavity axis the reconstruction works very well with an accuracy of $w_0/30 \approx 1\ \mu$m, which happens to be of the order of an optical wavelength.

The proposed detector arrangement was chosen to allow for easy analytic integration of the field intensity over the detector area and is not optimzed for the best reconstruction results. It might be constructed by segment mirrors imaging onto an array of single-photon counting detectors. Direct imaging on a high-sensitive high-speed camera seems more practical. In this case one has to numerically generate the lookup table to identify the most probable atomic position for a given field distribution. The construction of a suited cavity will be challenging. Scatter, misalignment, and deformation of the high-reflectivity mirrors must be kept to a minimum to prevent breaking of the cylindrical symmetry, which could lift the frequency degeneracy of the modes by too large of an amount. In the cavity in Garching the three modes used in our numerical example lie within a range of 22κ. It seems reasonable to assume that for a specially built cavity a splitting smaller than κ is feasible.

An extension of the idea presented here is to use a cavity where modes with different longitudinal mode index are degenerate. In that case, one can choose a combination of modes with opposite parity to break the 180° rotation symmetry. An example is a LG mode with even m degenerate with another one with odd m. Alternative geometries involving many degenerate modes as of a confocal cavity proposed in Ref. [16], will eventually lead to a single field maximum near the position of the atom avoiding ambiguities in the reconstruction.

In summary, we have shown that a high-finesse microcavity could be used as a real-time single-particle detector with high spatial resolution. In contrast to conventional single-atom detection schemes, the cavity works as a phase-contrast microscope enhanced by the inherent multipath interference of the high-finesse cavity. The method does not rely on fluorescence, and hence can also work for particles without a closed optical transition. Using larger sets of higher-order modes results in the encoding of more information in the field pattern allowing one to obtain higher resolution and track several particles. The scheme presented here could be implemented for single atoms moving in presently available high-finesse cavities, but possible applications extend beyond this system. The method should, in principle, also be applicable to large (bio)molecules in vacuum or even in solution.

P. H. and H. R. acknowledge support by the Austrian Science Foundation FWF (Project No. P13435-TPH).

[1] H. Mabuchi, Q. A. Turchette, M. S. Chapman, and H. J. Kimble, Opt. Lett. **21**, 1393 (1996).
[2] P. Münstermann, T. Fischer, P. W. H. Pinkse, and G. Rempe, Opt. Commun. **159**, 63 (1999).
[3] J. J. Childs, K. An, M. S. Otteson, R. R. Dasari, and M. S. Feld, Phys. Rev. Lett. **77**, 2901 (1996).
[4] C. J. Hood, M. S. Chapman, T. W. Lynn, and H. J. Kimble, Phys. Rev. Lett. **80**, 4157 (1998).
[5] P. Münstermann, T. Fischer, P. Maunz, P. W. H. Pinkse, and G. Rempe, Phys. Rev. Lett. **82**, 3791 (1999).
[6] P. W. H. Pinkse, T. Fischer, P. Maunz, and G. Rempe, Nature (London) **404**, 365 (2000).
[7] C. J. Hood, T. W. Lynn, A. C. Doherty, A. S. Parkins, and H. J. Kimble, Science **287**, 1447 (2000).
[8] A. C. Doherty, A. S. Parkins, S. M. Tan, and D. F. Walls, Phys. Rev. A **56**, 833 (1997).
[9] P. Horak, G. Hechenblaikner, K. M. Gheri, H. Stecher, and H. Ritsch, Phys. Rev. Lett. **79**, 4974 (1997).
[10] P. W. H. Pinkse, T. Fischer, P. Maunz, T. Puppe, and G. Rempe, J. Mod. Opt. **47**, 2769 (2000).
[11] M. Gangl and H. Ritsch, Eur. Phys. J. D **8**, 29 (2000).
[12] A. C. Doherty *et al.*, Phys. Rev. A **63**, 013401 (2000).
[13] A. E. Siegman, *Lasers* (University Science Books, Mill Valley, CA, 1986).
[14] P. Domokos, P. Horak, and H. Ritsch, J. Phys. B **34**, 187 (2001).
[15] T. Fischer, P. Maunz, T. Puppe, P. W. H. Pinkse, and G. Rempe, New J. Phys. **3**, 11.1 (2001).
[16] S. E. Morin, C. C. Yu, and T. W. Mossberg, Phys. Rev. Lett. **73**, 1489 (1994).